

## FLING IN NEAR-FAULT GROUND MOTIONS AND ITS EFFECT ON STRUCTURAL COLLAPSE CAPACITY

Lynne S. Burks<sup>1</sup> and Jack W. Baker<sup>2</sup>

<sup>1</sup> Sandia National Labs, Livermore, CA

<sup>2</sup> Dept. of Civil & Environmental Engineering, Stanford University, Stanford, CA

### Abstract

We evaluate the collapse capacity of a nonlinear single degree of freedom (SDOF) system using ground motion records with varying fling properties, including records with static offsets preserved via baseline correction, records with static offsets removed via filtering, and records with artificial static offsets added. Fling is caused by a permanent static offset of the ground and appears as a ramp function in the displacement time history. Due to baseline errors in many acceleration recordings, these static offsets are typically removed via filtering before ground motion records are added to an engineering database, such as the Next Generation Attenuation (NGA) database. Therefore, fling is neglected by default in many engineering applications even though it may affect the dynamic nonlinear response of structures, extreme nonlinear behavior such as collapse, and structures crossing a fault. Some analysts account for fling by adding artificial static offsets to filtered records, but this method has not been rigorously tested and there has been little study on the effects of fling on nonlinear structural behavior and collapse capacity. We found that the collapse capacity of a degrading nonlinear SDOF is similar for two versions of the same ground motion: one with the static offset preserved via baseline correction and one with the static offset removed via filtering. In most cases, the baseline corrected record and the filtered record result in the same collapse capacity, indicating that filtering preserves the dynamic effect of fling even though the static offset is removed. We also found that adding artificial static offsets to filtered records typically results in a conservative estimate of the collapse capacity. In particular, increased amplitude, or static offset, and decreased period, or duration of fling, cause decreased collapse capacity.

### Introduction

Near-fault effects, such as directivity and fling, tend to produce intense structural response because of ground motion amplification at long periods [1]. Directivity is caused by the constructive interference of seismic waves as the rupture propagates along the fault and is strongest in the fault normal direction. Fling is caused by a permanent static offset of the ground and is strongest for strike-slip faults in the fault parallel direction. While directivity has received much attention by structural engineers, fling has been largely ignored because static offsets are typically filtered out of ground motion records before being used for engineering analysis.

---

This document is reprinted from: Burks, Lynne S., and Jack W. Baker. Fling in near-fault ground motions and its effect on structural collapse capacity. *Proceedings of the 10<sup>th</sup> National Conference in Earthquake Engineering*, Earthquake Engineering Research Institute, Anchorage, AK, 2014.

Raw seismograms recorded from earthquakes contain errors due to noise and baseline offsets from tilting and transducer response to strong shaking. These errors in acceleration are significantly amplified when integrated twice to compute displacement, so analysts address this by processing ground motion records using filtering and baseline correction (Figure 1). Filtering consists of applying a low- and high-pass filter in the frequency domain, and typically removes the static offset from records [2]. Baseline correction removes baseline offsets by fitting and then subtracting a linear trend from the velocity time history, and preserves the static offset [3,4]. However, because the amplitude of the static offset is highly sensitive to the choice of baseline, and baseline correction has a negligible effect on elastic response spectra [3,5], records are typically filtered rather than baseline corrected before being added to an engineering database, such as the Next Generation Attenuation (NGA) database [6].

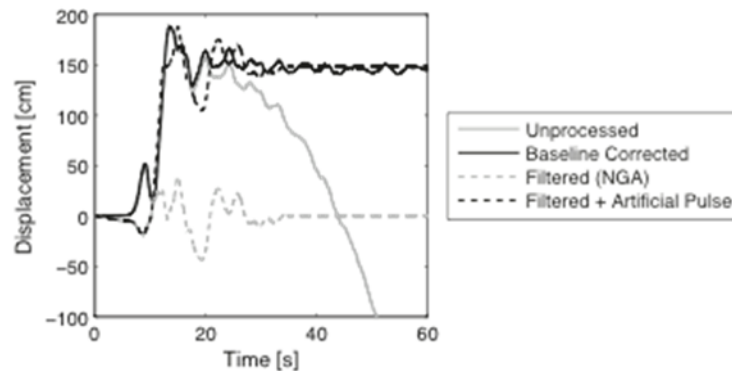


Figure 1. Multiple versions of the displacement time history from the YPT station in the 1999 Kocaeli, Turkey earthquake, including unprocessed (or raw), baseline corrected, filtered (from NGA database), and filtered plus an artificial fling pulse.

Previous studies show that the structural response to near-field and pulse-like ground motions is generally more intense than to far-field ground motions, especially when the pulse period is close to the first or second mode period of the structure, e.g. [7–9]. Some analysts account for this effect by adding artificial fling pulses to filtered ground motions (e.g. Figure 1) [10], but this method neglects the difference in record processing techniques like filtering and baseline correction, which may affect structural response [11]. Also, previous studies do not address the effect of fling on collapse capacity, which is becoming an increasingly important parameter for the assessment of highly nonlinear structures and seismic risk analysis.

Here we compare the collapse capacity of nonlinear SDOF structures using records with static offsets preserved via baseline correction, static offsets removed via filtering from the NGA database, and static offsets included via adding artificial pulses to the filtered NGA record. We find that the baseline corrected record and the filtered record result in similar collapse capacity, and that adding artificial pulses generally decreases the collapse capacity.

## Ground Motions

We first consider three types of idealized pulses because though many parametric studies have been done using idealized pulses, e.g. [12–15], none specifically focus on collapse capacity. Then we assess collapse capacity using many variations of three recorded ground motions.

### Idealized Pulses

The three idealized pulses are referred to as type *A*, type *B*, and type *C*, where type *A* and type *C* represent fling and type *B* represents a directivity pulse with no static offset (Figure 2). Each pulse is represented by a trigonometric function as follows [15]:

$$a_A(t) = \frac{2\pi D_p}{T_p^2} \sin\left(\frac{2\pi}{T_p}(t-t_1)\right) \quad t_1 \leq t < T_p + t_1 \quad (1)$$

$$a_B(t) = \frac{2\pi^2 D_p}{T_p^2} \cos\left(\frac{2\pi}{T_p}(t-t_1)\right) \quad t_1 \leq t < T_p + t_1 \quad (2)$$

$$a_C(t) = -\frac{\pi^2 D_p}{2T_p^2} \sin\left(\frac{\pi}{T_p}\left(t-t_1-\frac{T_p}{2}\right)\right) \quad t_1 \leq t < T_p + t_1 \quad (3)$$

where  $a_A(t)$ ,  $a_B(t)$ , and  $a_C(t)$ , are the acceleration as a function of time for pulse *A*, *B*, and *C*, respectively,  $D_p$  is the maximum displacement amplitude of the pulse,  $T_p$  is the period or duration of the pulse, and  $t_1$  is the arrival time.

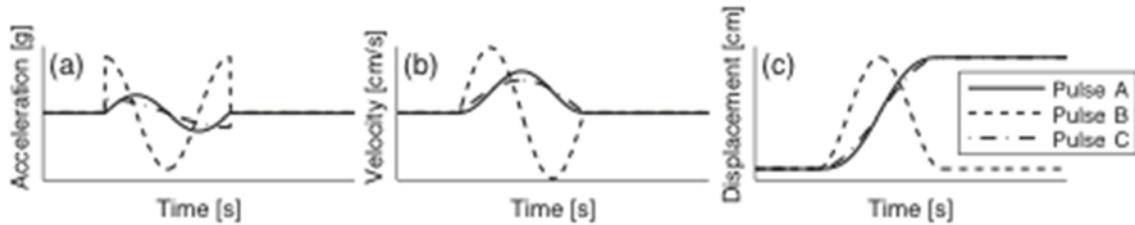


Figure 2. (a) Acceleration, (b) velocity, and (c) displacement time histories of different types of idealized pulses.

We used 40 versions of each pulse type with constant maximum acceleration of the pulse,  $A_p$ , and varying  $T_p$  (Figure 3). Each set of pulses was also high-pass filtered at a cutoff frequency,  $f_c$ , of 0.2 Hz and 0.5 Hz to investigate the effect of record filtering on collapse capacity.

### Ground Motion Recordings

We also consider three recorded ground motions: the TCU068-N/S station from the 1999 Chi-Chi, Taiwan earthquake; the GDLC-E/W station from the 2010 Darfield, New Zealand

earthquake; and the YPT-N/S station from the 1999 Kocaeli, Turkey earthquake. These stations have a Joyner-Boore distance of 0, 1.22, and 1.38 km respectively. For each recording, we used a version with static offsets preserved via baseline correction, static offsets removed via filtering from the NGA database [6], and artificial static offsets included via adding pulse  $C$  with varying fling parameters (displacement amplitude, pulse period, and arrival time) to the filtered version.

For the version with static offsets preserved, we performed baseline correction according to [3] and [4] on raw seismograms from the TCU068 [16], GDLC [17], and YPT stations (Erol Kalkan, personal communication, May 2011). We then fit the functional form for pulse  $C$  to each baseline corrected displacement time history using global optimization (for more details, see [18]). Fling parameters of the baseline corrected ground motions are shown in

Table 1.

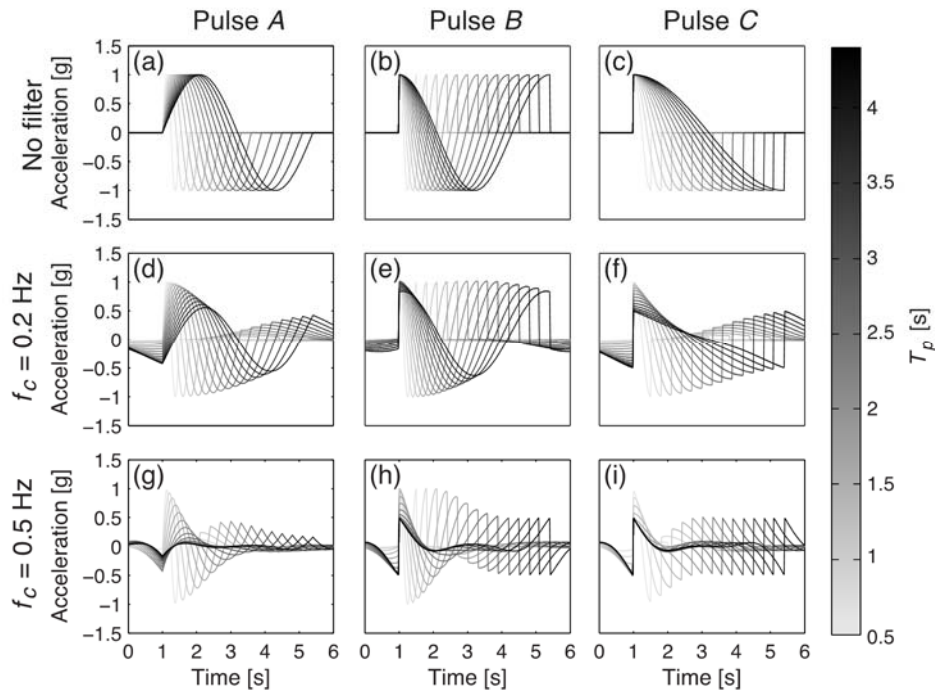


Figure 3. Acceleration time histories of selected pulses used to compute collapse capacity.

 Table 1. Fling parameters of the baseline corrected versions of the three ground motion records used in this study, where  $D_p$  is displacement amplitude,  $T_p$  is pulse period, and  $t_l$  is arrival time.

EQ Name	Year	$M_W$	Station Name	Orientation	$D_p$ (cm)	$T_p$ (s)	$t_l$ (s)
Chi-Chi	1999	7.6	TCU068	N/S	551.0	3.19	33.9
Darfield	2010	7.0	GDLC	E/W	134.2	3.37	17.9

---

Kocaeli	1999	7.5	YPT	N/S	148.4	2.84	10.2
---------	------	-----	-----	-----	-------	------	------

---

For the versions with artificial static offsets included, we computed many displacement time histories of pulse  $C$  (using Equation 3) with varying  $D_p$ ,  $T_p$ , and  $t_l$ . We varied each fling parameter 40 times while holding the other two parameters constant, resulting in a total of 120 pulse  $C$  displacements for each recording. We then added the pulse  $C$  displacements to each filtered NGA recording, representing the way that some analysts add artificial fling to filtered near-fault records [10,19]. Multiple versions of the ground motion from TCU068 with varying  $D_p$  are shown in Figure 4. Similarly,  $T_p$  and  $t_l$  were also varied for TCU068, and all fling parameters were varied for GDLC and YPT, but figures are omitted here because of space constraints (see [18]).

### Structural Analysis

Here we present the results of an incremental dynamic analysis (IDA) performed in OpenSees using ground motions from the previous section. An IDA is performed by incrementally scaling up a single ground motion and computing a structural demand parameter, like interstory drift or floor acceleration, until instability and collapse occurs. The IDA is repeated for a set of ground motions to get a probabilistic description of collapse [20].

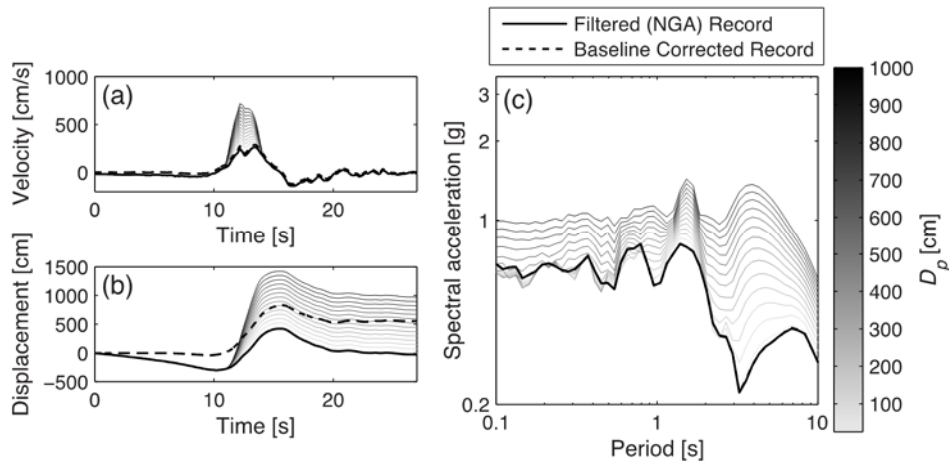


Figure 4. Selected versions of the (a) velocity time history, (b) displacement time history, and (c) response spectra of the ground motion recorded at the TCU068 station during the 1999 Chi-Chi, Taiwan earthquake with varying  $D_p$ .

### Structures

For this study, we used two nonlinear single degree of freedom (SDOF) structures with different fundamental periods and force-drift backbones which capture the collapse behavior of the structure (Figure 5). SDOF 1 has a natural period of 1.32 s and is based on a SDOF approximation of a 4-story experimental structure [21]. SDOF 2 has a longer period of 3 seconds, which is closer to observed pulse periods from the recorded ground motions. Both SDOFs have a 2% damping ratio and 3% strain hardening ratio.

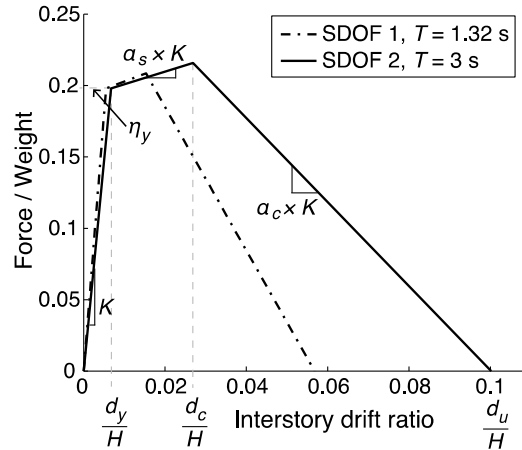


Figure 5. Force-drift backbone of the nonlinear and degrading SDOF structures used in this study, where  $\eta_y$  is yield force normalized by weight,  $K$  is stiffness,  $\alpha_s$  is strain hardening ratio,  $\alpha_c$  is post-capping stiffness ratio,  $H$  is SDOF height,  $d_y$  is yield displacement,  $d_c$  is capping displacement, and  $d_u$  is ultimate displacement.

### Response to Idealized Pulses

The idealized pulse ground motions were used to perform multiple IDAs on SDOF 1, with ground motions grouped by pulse type and filter cutoff frequency (Figure 6). The filter cutoff frequency of 0.2 Hz has a negligible effect on the collapse capacity for all pulse types, while the cutoff frequency of 0.5 Hz causes an increase in collapse capacity for all pulse types. This increase is likely due to the decrease in energy of the pulses from filtering.

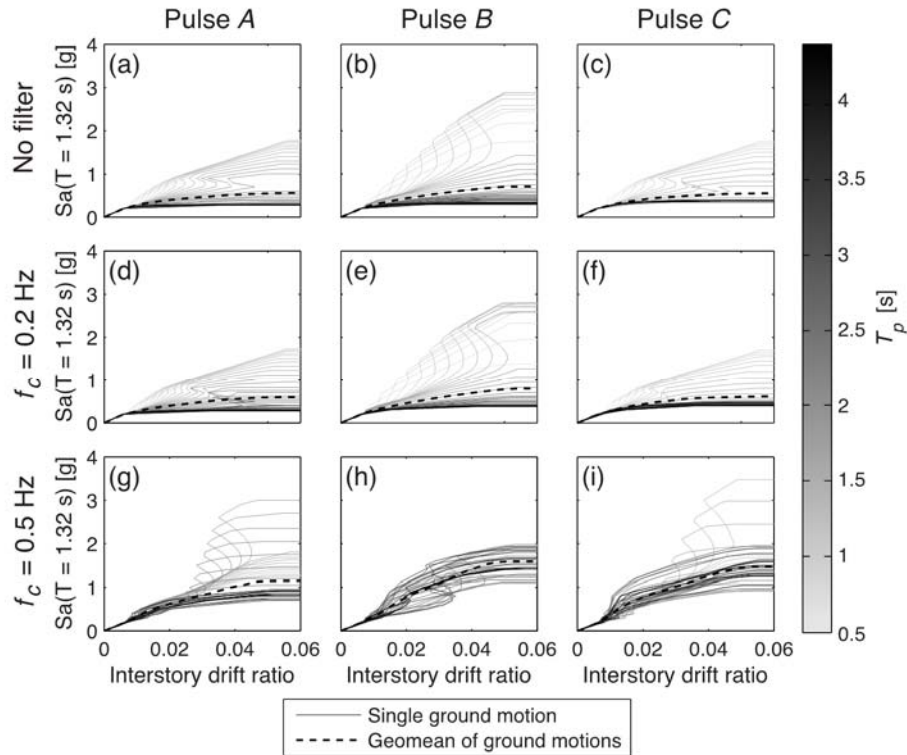


Figure 6. Results of IDA performed on SDOF 1 using idealized pulses with varying filter frequency shown in Figure 3.

## Response to Ground Motion Recordings

The collapse capacity of SDOF 1 was computed using all versions of the record from TCU068 (Figure 7), GDLC, and YPT. Because of space constraints, only results from TCU068 are presented here, but the other ground motions show similar trends [18]. For all three records, the version with static offsets preserved via baseline correction and the version with static offsets removed via filtering from the NGA database resulted in similar collapse capacity. This indicates that even though the static offset is removed from the NGA version, the dynamic component of fling is preserved. Also, for most records and fling parameters, adding pulse C to the filtered NGA version resulted in decreased collapse capacity. But there were a few notable exceptions where the collapse capacity increased, such as some small displacement amplitudes for the TCU068 record and very short periods for all records.

To investigate possible reasons for the increased collapse capacity, we evaluated the displacement of SDOF 1 as a function of time at varying scale factors until collapse. For the filtered version of the Chi-Chi record, the residual displacement of the SDOF increased with scale factor until collapse occurred in the positive direction (Figure 8a). But when pulse C with  $D_p = 375$  cm was added to the filtered version, the residual displacement decreased with scale factor before collapse occurred again in the positive direction, indicating that the pulse pulled the SDOF in the negative direction (Figure 8b). For some ground motions, such as pulse C with a very short period of 1 s added to the filtered version, this pull was strong enough to cause collapse in the negative direction (Figure 8c). In this example, we observed that the added pulse

pulled the SDOF in the opposite direction of the filtered record, sometimes causing collapse in the opposite direction, and always increasing the collapse capacity.

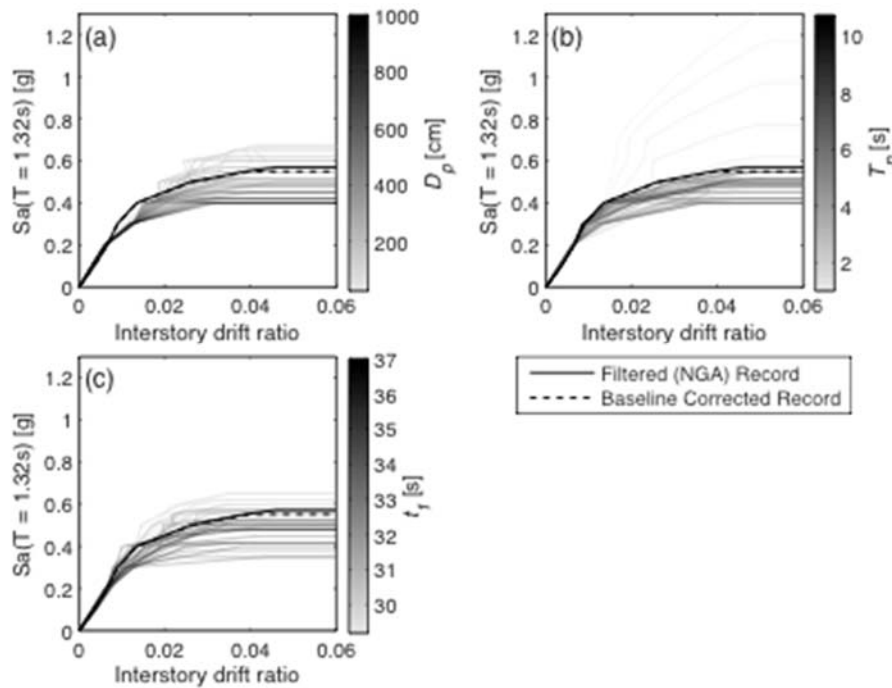


Figure 7. Collapse capacity of SDOF 1 computed using multiple versions of the TCU068 Chi-Chi, Taiwan ground motion, including with static offsets preserved via baseline correction, static offsets removed via filtering from the NGA database, and static offsets included via adding pulse  $C$  with varying (a)  $D_p$ , (b)  $T_p$ , and (c)  $t_1$  to the NGA version.

General trends between parameters of the added pulse  $C$  and collapse capacity were observed. For example, as  $D_p$  increased or  $T_p$  decreased, the collapse capacity generally decreased, but no such trend was observed for  $t_1$  (Figure 9). For each ground motion with added pulse  $C$ , we compared the difference between the pulse  $C$  and baseline corrected fling parameters to the ratio of the collapse capacity from the filtered version with added pulse  $C$  to the collapse capacity from the baseline corrected version. When the difference between fling parameters (i.e. the x-axis of Figure 9) is zero, we are comparing the baseline corrected version to the filtered version added to pulse  $C$  with the same fling parameters as the baseline corrected version, and their resulting collapse capacities are not equal. This inequality indicates that adding a fling pulse to the filtered version, even with the “correct” parameters (i.e. parameters same as the baseline corrected version), double counts the effect of fling and causes a conservative estimate of collapse capacity.

We also computed the collapse capacity for SDOF 2 using all versions of the ground motion records, but because the general conclusions are similar to SDOF 1, we only show the results from Darfield in summary form for conciseness (Figure 9). Even though the natural period of SDOF 2 is closer to  $T_p$  for all three records, the baseline corrected and filtered versions again result in similar collapse capacity. The versions with static offsets included via adding

pulse  $C$  to the filtered version nearly always result in decreased collapse capacity. Finally, we again observed that as  $D_p$  increased or  $T_p$  decreased, the collapse capacity generally decreased.

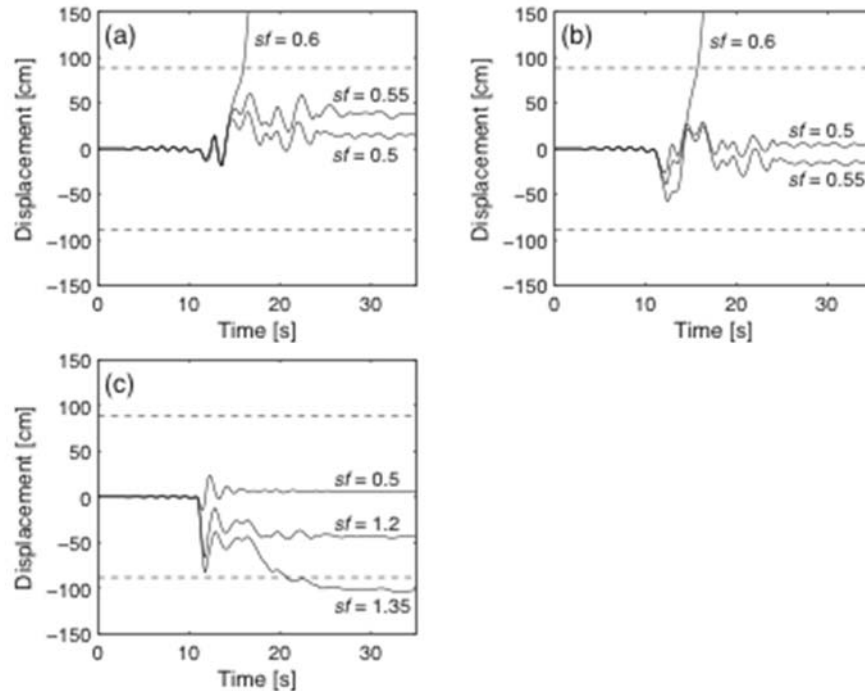


Figure 8. Displacement response of SDOF 1 to multiple versions of the TCU068 Chi-Chi, Taiwan ground motion record scaled at different factors (where  $sf$  is the scale factor), including (a) the NGA version, (b) pulse  $C$  with  $D_p = 375$  cm added to the NGA version, and (c) pulse  $C$  with  $T_p = 1$  s added to the NGA version. Collapse occurs when the displacement of SDOF 1 exceeds the ultimate displacement represented by the dashed line.

## Conclusions

We computed the collapse capacity of nonlinear SDOFs using multiple versions of the same ground motion record, including a baseline corrected version with static offsets preserved, a filtered version from the NGA database with static offsets removed, and artificial versions with an idealized pulse added to the filtered record. For all records and two SDOFs with different periods, the baseline corrected and filtered versions resulted in similar collapse capacity. This indicates that even when the static offset is removed via filtering, the dynamic effect of the fling on these structures is preserved. Collapse capacities were considered in this study in order to evaluate fling effects on highly nonlinear structures. Similar conclusions have been drawn for linear SDOFs [5], and these studies indicate that moderately nonlinear structural responses will likely also be insensitive to record processing that removes static fling.

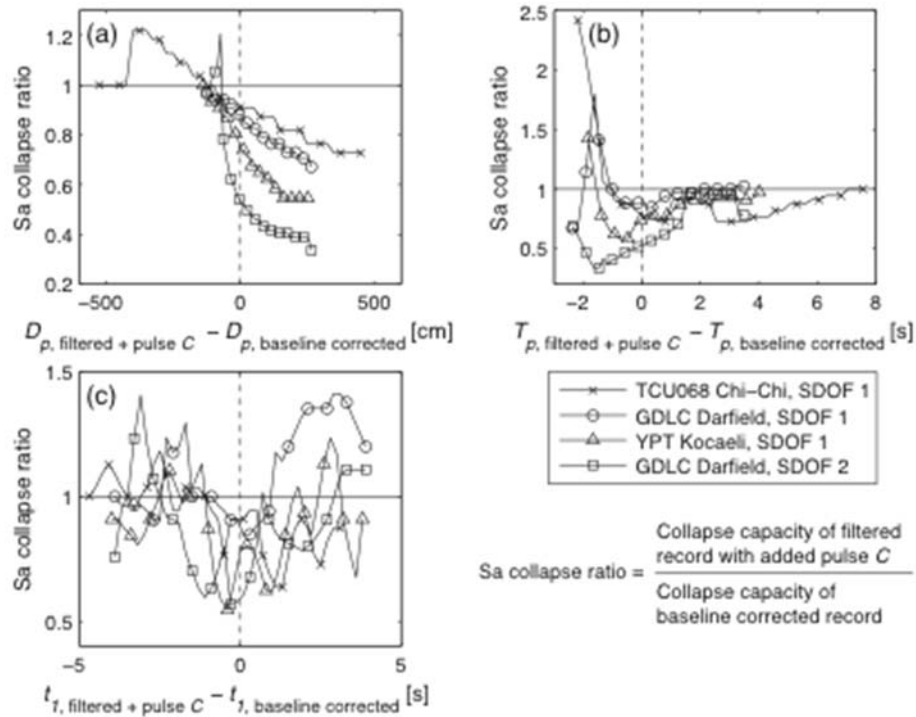


Figure 9. Changes in fling parameter affect the collapse capacity. The x-axis is the difference between (a)  $D_p$ , (b)  $T_p$ , and (c)  $t_l$  of the filtered version with added pulse  $C$  and the baseline corrected version. The y-axis is the ratio of the collapse capacity of the filtered version with added pulse  $C$  to the baseline corrected version.

We also evaluated the effect of ground motion filtering on collapse capacity through idealized pulse approximations of fling and directivity. By computing collapse capacities for a range of pulse periods and high-pass filter cutoff frequencies, we concluded that filtering at a low cutoff frequency outside the range of pulse or structural periods has a negligible effect on collapse capacity. But filtering at a high cutoff frequency that approaches the pulse or structural period can increase the collapse capacity, leading to an un-conservative estimate.

By adding artificial fling pulses to filtered records, we observed that as displacement amplitude increased or pulse period decreased, the collapse capacity typically decreased. No such trend was found for the arrival time of the fling pulse. Adding any artificial fling pulse to a filtered record typically resulted in a conservative estimate of collapse capacity. But in a few cases, the artificial fling pulled the SDOF in the opposite direction of the filtered record, sometimes even causing collapse in the opposite direction, and resulted in an un-conservative estimate of collapse capacity.

In conclusion, the collapse capacity of a nonlinear SDOF is similar whether computed with a filtered or baseline corrected version of the ground motion, so either can be used in applications similar to the examples presented here. However, fling may still be important for other engineering applications, such as fault crossings where the main problem is static displacement rather than dynamic response.

## References

- [1] Somerville PG, Smith NF, Graves RW, Abrahamson NA. Modification of Empirical Strong Ground Motion Attenuation Relations to Include the Amplitude and Duration Effects of Rupture Directivity. *Seismological Research Letters* 1997; **68** (1): 199–222.
- [2] Boore DM, Bommer JJ. Processing of strong-motion accelerograms: needs, options and consequences. *Soil Dynamics and Earthquake Engineering* 2005; **25**: 93–115.
- [3] Boore DM. Effect of Baseline Corrections on Displacements and Response Spectra for Several Recordings of the 1999 Chi-Chi, Taiwan, Earthquake. *Bulletin of the Seismological Society of America* 2001; **91** (5): 1199–1211.
- [4] Wu Y-M, Wu C-F. Approximate recovery of coseismic deformation from Taiwan strong-motion records. *Journal of Seismology* 2007; **11**: 159–170.
- [5] Kamai R, Abrahamson N. Are Fling Effects Captured in the New NGA West2 Ground Motion Models? *Earthquake Spectra* 2014; in press.
- [6] Chiou B, Darragh R, Gregor N, Silva W. NGA Project Strong-Motion Database. *Earthquake Spectra* 2008; **24** (1): 23–44.
- [7] Alavi B, Krawinkler H. Effects of near-fault ground motions on frame structures 2001; Blume Earthquake Engineering Center Technical Report 138; Stanford, CA.
- [8] Kalkan E, Kunnath SK. Effects of Fling Step and Forward Directivity on Seismic Response of Buildings. *Earthquake Spectra* 2006; **22** (2): 367–390.
- [9] Calugaru V, Panagiotou M. Response of tall cantilever wall buildings to strong pulse type seismic excitation. *Earthquake Engineering & Structural Dynamics* 2012; **41** (9): 1301–1318.
- [10] Stewart JP, Chiou SJ, Bray JD, Graves RW, Somerville PG, Abrahamson NA. Ground Motion Evaluation Procedures for Performance-Based Design 2001; Pacific Earthquake Engineering Research Center Technical Report 2001/09; Berkeley, CA.
- [11] Ventura CE, Archila M, Bebamzadeh A, Liam Finn WD. Large coseismic displacements and tall buildings. *The Structural Design of Tall and Special Buildings* 2011; **20**: 85–99.
- [12] Makris N. Rigidity–Plasticity–Viscosity: Can Electrorheological Dampers Protect Base-Isolated Structures from Near-Source Ground Motions? *Earthquake Engineering & Structural Dynamics* 1997; **26** (5): 571–591.
- [13] Makris N, Roussos YS. Rocking response of rigid blocks under near-source ground motions. *Géotechnique* 2000; **50** (3): 243–262.
- [14] Makris N, Black CJ. Dimensional Analysis of Bilinear Oscillators under Pulse-Type Excitations. *Journal of Engineering Mechanics* 2004; **130** (9): 1019–1031.
- [15] Makris N, Black CJ. Dimensional Analysis of Rigid-Plastic and Elastoplastic Structures under Pulse-Type Excitations. *Journal of Engineering Mechanics* 2004; **130** (9): 1006–1018.

- [16] Lee WHK, Shin TC, Kuo KW, Chen KC, Wu CF. CWB Free-Field Strong-Motion Data from the 921 Chi-Chi Earthquake: Processed Acceleration Files on CD-ROM 2001; Central Weather Bureau; Taipei, Taiwan.
- [17] CESMD. Center for Engineering Strong Motion Data [Internet]. *Strong Motion Archive* 2014; Available from: [www.strongmotioncenter.org](http://www.strongmotioncenter.org)
- [18] Burks LS. Ground motion simulations: validation and application for civil engineering problems 2014; Stanford University Ph.D. Thesis; Stanford, CA.  
<http://purl.stanford.edu/rr972yp3813>
- [19] Abrahamson NR. Velocity Pulses in Near-Fault Ground Motions 2002; In: CUREE Symposium; Berkeley, CA.
- [20] Ibarra LF, Krawinkler H. Global collapse of frame structures under seismic excitations 2005; Blume Earthquake Engineering Center Technical Report 152; Stanford, CA.
- [21] Lignos D, Krawinkler H, Whittaker AS. Prediction and validation of sidesway collapse of two scale models of a 4-story steel moment frame. *Earthquake Engineering & Structural Dynamics* 2011; **40**: 807–825.